Coherent optical OFDM scheme with inter-carrier interference self-cancellation and common phase error compensation

Yiling Wu (吴毅凌), Juhao Li (李巨浩), Chunxu Zhao (赵春旭), Yuping Zhao (赵玉萍)*, Fan Zhang (张 帆), and Zhangyuan Chen (陈章渊)

State Key Laboratory of Advanced Optical Communication Systems & Networks, Peking University, Beijing 100871, China

**E-mail: yuping.zhao@pku.edu.cn*

Received December 28, 2009

Schemes integrating inter-carrier interference (ICI) self-cancellation and common phase error (CPE) compensation for coherent optical orthogonal frequency division multiplexing (CO-OFDM) systems are investigated. The purpose of our research is to counteract the impacts of laser phase noise and fiber nonlinearity. We propose two ICI self-cancellation-based CO-OFDM schemes, and adopt a pilot-aided decision feedback (DFB) loop for CPE compensation. The proposed schemes are compared with conventional CO-OFDM schemes at the same spectral efficiency. Simulations show that our schemes can not only enhance laser linewidth tolerance of the CO-OFDM system, but also present strong robustness against fiber nonlinearity.

OCIS codes: 060.2330, 060.4080, 060.1660.

doi: 10.3788/COL20100807.0634.

Tremendous advances in the semiconductor technology have resulted in studies on electronic dispersion compensation since the early 1990s, particularly, to enhance optical communication system performance[1,2]. Orthogonal frequency division multiplex (OFDM) techniques have recently attracted much attention[3−6]. The optical OFDM system is robust against interference caused by chromatic dispersion (CD) and polarization-mode dispersion (PMD) in optical fiber transmission[7,8]. Compared with direct-detection optical OFDM (DD-OOFDM) systems, the coherent optical OFDM (CO-OFDM) system is more suitable for long-haul transmission due to its higher spectral and power efficiency[9]. Experimental results have shown that the CO-OFDM system is practical for long-haul transmission at the rate of tens of gigabits[10,11]. CO-OFDM techniques for long-haul transmission of 100-Gb/s-class channels have been described and tested in Ref. [12].

OFDM systems are sensitive to carrier frequency offset (CFO) and phase noise. They introduce two kinds of impacts to OFDM signals, which are also referred to as inter-carrier interference (ICI) and common phase error (CPE)[13,14]. ICI behaves like an additive Gaussian noise while CPE rotates the phase of all constellation points in a common direction. Phase noise contributed by the transmitter and receiver laser significantly degrades the performance of CO-OFDM systems[15]. Some methods that have been proposed to combat laser phase noise include radio frequency (RF) pilot-aided phase noise compensation and self-optical carrier extraction[16,17]. Both transmit a RF-pilot tone together with the OFDM signal, and use the extracted RF-pilot at the receiver for down-conversion. Aside from laser phase noise, fiber nonlinearity introduces large distortions to optical OFDM signals, such as self-phase modulation (SPM) and inter-sub-carrier crosstalk[18,19]. Both pre-compensation and partial carrier filling (PCF) schemes, as proposed in Refs. [20, 21], respectively, show robustness against fiber nonlinearity.

To solve the problem, we study the ICI self-cancellation and CPE compensation methods for CO-OFDM systems. Then, zero-padding and data-conversion ICI self-cancellation methods are investigated and compared[22]. The two methods can not only obtain lower ICI levels, but also suppress inter-sub-carrier crosstalk caused by fiber nonlinearity. To compensate the CPE, we employ a pilot-aided decision feedback (DFB) loop, which could also eliminate SPM effect caused by fiber nonlinearity.

As an effect of laser phase noise or residual CFO, the received OFDM signal can be expressed as[13,14]

$$R_m(n) = X_m(n)H_m(n)I_m(0) + \sum_{l=0,l\neq n}^{N-1} X_m(l)H_m(l)I_m(l-n) + Z_m(n), \quad (1)$$

where n denotes sub-carrier index and $0 \leq n \leq N-1$; N is total number of sub-carriers; $X_m(n)$ is signal transmitted on the nth sub-carrier of the mth OFDM symbol; $H_m(n)$ is the channel frequency response of the nth sub-carrier; $Z_m(n)$ is Gaussian noise. $I_m(l-n)$ represents the ICI term caused by phase noise or residual CFO. If only the OFDM signal is affected by laser phase noise, $I_m(l-n)$ can be expressed as[13]

$$I_m(l-n) = \frac{1}{N}\sum_{n=0}^{N-1} \mathrm{e}^{\mathrm{j}\phi_m(n)} \cdot \mathrm{e}^{\mathrm{j}\frac{2\pi(l-n)n}{N}}, \quad (2)$$

where $\phi_m(n)$ is phase noise on the nth sample of the mth OFDM symbol.

From Eq. (1), laser phase noise produces two kinds of interference to the OFDM signal. The first term on the right of Eq. (1) stands for CPE with $I_m(0)$ representing the CPE coefficient. The second item stands for the ICI

with $I_m(l-n)$ representing the ICI coefficient between the lth and nth sub-carriers.

ICI self-cancellation technique was initially proposed to combat ICI caused by CFO[22]. Since ICI caused by phase noise has similar characteristics to that caused by CFO, the ICI self-cancellation technique is also effective for the latter[15,23]. Based on these investigations, we propose to introduce ICI self-cancellation technique into the CO-OFDM system. In this letter, two ICI self-cancellation methods are investigated.

The amplitude of $I_m(l-n)$ changes gradually from one to the next, and the $(n-1)$th and $(n+1)$th sub-carriers produce larger ICI to the nth sub-carrier compared with the others[22,23]. Thus, we reduced ICI by assigning zero values to one of every two adjacent sub-carriers. Then, the transmitted signal was expressed as

$$X_m(n) = \begin{cases} D_m(n/2), & n \text{ is even} \\ 0, & \text{otherwise} \end{cases}, \tag{3}$$

where $D_m(k)$ denotes the kth data symbol transmitted in the mth OFDM symbol. This scheme has been referred to as "zero-padding" ICI self-cancellation. Figure 1(a) demonstrates the sub-carrier assignment of the scheme.

Zhao *et al.* proposed an ICI self-cancellation scheme in which one transmitted data symbol was mapped onto two adjacent sub-carriers with opposite weight[22]. The transmitted signal was expressed as

$$X_m(n) = \begin{cases} D_m(n/2), & n \text{ is even} \\ -D_m(n/2), & \text{otherwise} \end{cases}. \tag{4}$$

This scheme has been referred to as "data-conversion" ICI self-cancellation. Figure 1(b) demonstrates the sub-carrier assignment of the scheme. As described in Ref. [22], the ICI cancellation demodulation was implemented after channel equalization at the receiver. In doing so, we used $y_m(n)$ to denote the equalized signal on the nth sub-carrier of the mth OFDM symbol. The output of the ICI cancellation demodulator was then expressed as

$$Y'_m(k) = [Y_m(2k) - Y_m(2k+1)]/2, \tag{5}$$

where k=0, 1, $\cdots$, $N/2-1$.

From Eq. (1), the CPE coefficient $I_m(0)$ remained unchanged for all subcarriers in one OFDM symbol. It was possible to estimate the phase of $I_m(0)$ in each OFDM; the data- and pilot-aided phase estimation methods for the CO-OFDM system were discussed in Ref. [24]. However, data-aided methods were rather limited by phase ambiguity, which could result in larger phase estimation error during strong phase noise. Even if the pilot-aided method could avoid the same problem, pilots might consume the useful bandwidth and lower the transmission efficiency of the communication system. The estimation accuracy of the pilot-aided method decreased with the number of pilot sub-carriers.

To improve the performance of the phase estimation, we proposed a pilot-aided DFB loop that combined pilot- and data-aided methods. The CPE of the mth OFDM symbol was estimated as

$$\Phi_m = \frac{1}{N}\sum_{n=0}^{N-1}\left\{\arg\left[R_m(n)\right] - \arg\left[\tilde{X}_m(n)\right]\right\}, \tag{6}$$

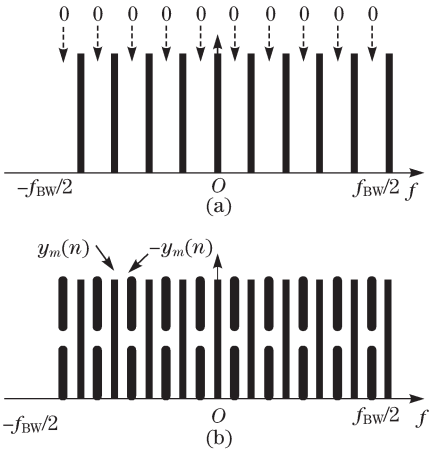

Fig. 1. Demonstration of the sub-carrier assignment for the zero-padding and the data-conversion ICI self-cancellation schemes: (a) zero-padding and (b) data-conversion.

where arg[·] is the calculation of the phase angle. For the data sub-carrier, $\tilde{X}_m(n)$ denotes the estimated transmitted data symbol; for the pilot sub-carrier, $\tilde{X}_m(n)$ denotes the known transmitted pilot symbol. Compared with the Mth-power-law method used by the data-aided CPE compensation scheme described in Ref. [24], we employed a DFB loop to estimate the CPE of the data sub-carrier to avoid phase ambiguity. However, any wrong decision of the received signal would lower the accuracy of the DFB loop since decisions were initially assumed as correct. To solve the problem, we used several pilots to confirm the range of the CPE and to exclude inaccurate estimation results that were provided by the wrong decision. Since all sub-carriers were used for phase estimation, the proposed pilot-aided DFB loop achieved higher accuracy compared with the pilot-aided method.

The optical OFDM system was sensitive to fiber nonlinearity due to the high peak-to-average power ratio (PAPR) of the OFDM signal. The impact of fiber nonlinearity was somewhat similar to that of laser phase noise. Inter-sub-carrier crosstalk caused coherent interference between adjacent sub-carriers, which could be viewed as a kind of ICI. Meanwhile, the SPM rotated the phase of transmitted signal in a common direction, a behavior similar to CPE.

The PCF technique was effective in reducing inter-sub-carrier crosstalk generated by fiber nonlinearity[20]. In the PCF scheme, redundant zero values were assigned to a certain OFDM sub-carrier. By adopting a proper carrier-filling pattern, most of inter-sub-carrier crosstalks would locate into the unfilled (zero) sub-carriers. Consequently, interference on the filled (data) sub-carriers significantly decreased. When the zero-padding ICI self-cancellation scheme was adopted in the CO-OFDM system, zero value was assigned to one of every two adjacent sub-carriers. The carrier-filling pattern is shown in Fig. 1(a). This pattern was effective in reducing the impact of inter-sub-carrier crosstalk. In addition, the pilot-aided DFB loop was effective in compensating phase rotation in a common direction caused by SPM.

Figure 2 shows the structure of the CO-OFDM simulation system. At the transmitter, data bits were encoded onto baseband OFDM signals, after which an optical in-

phase/quadrature (I/Q) modulator was used to convert directly the baseband signal into the optical domain. During fiber nonlinearity simulation, a transmission link consisting of 30 spans was employed. Each included 80-km standard single mode fibers (SSMF) with chromatic dispersion coefficients of 16 ps/(nm·km), 12.8-km dispersion compensation fibers (DCF) with chromatic dispersion coefficients of −100 ps/(nm·km), and Er-doped fiber amplifiers (EDFAs), to compensate for fiber loss and noise of 4 dB. Both SSMF and DCF obtained nonlinear coefficients of γ=1.31 $W^{-1}\cdot km^{-1}$ and effective areas of 35 and 80 μm^2, respectively, when the fiber nonlinearity was emulated. The optical band-pass filter (OBPF) had a bandwidth of 50 GHz. The coherent receiver consisted of a 90° hybrid in which the received signal and a local oscillator (LO) were shown to interfere before they were detected by two balanced detectors. OFDM signals were decoded into the data bits by the OFDM decoder. Electrical low-pass filters (LPFs) were square-root-raised to cosine filters with a roll-off factor of 0.2. At the receiver, after synchronization, the signal was equalized in the frequency domain. The phase of each block was first corrected by using pilots and then averaged by using the Viterbi-Viterbi method.

Binary phase shif keying (BPSK) was used for the conventional CO-OFDM system. Since both zero-padding and data-conversion methods used only half on the subcarriers for data transmission, quadrature phase shift keying (QPSK) was used for two ICI self-cancellation to evaluate the advantage of the proposed scheme at the same spectral efficiency. To remove the impact of the modulation format on the fiber nonlinearity tolerance, the performance of the conventional CO-OFDM system with QPSK modulation was also simulated. For conventional CO-OFDM scheme, mapped BPSK or QPSK signals were grouped into blocks with 248 symbols each, and 8 pilots were multiplexed into each block. For the proposed schemes, 256 zeros or opposite numbers were inserted evenly. For the conventional method, the cyclic prefix (CP) with an 8-sample length was inserted for each block. The CP with 16-sample length was incorporated into the proposed schemes. The preamble included 4 Chu-sequences for channel estimation.

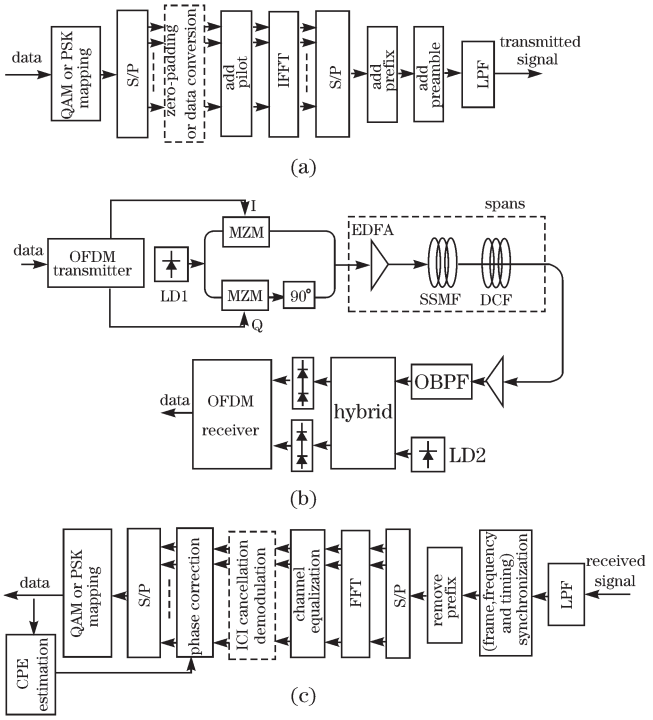

Fig. 2. Structure of the simulation system. (a) Structure of baseband OFDM transmitter, (b) conceptual diagram of CO-OFDM system, and (c) structure of baseband OFDM receiver. QAM: quadrature amplotude modulation; PSK: phase shift keying; S/P: serial-to-parallel; IFFT: inverse fast Fourier transform; P/S: parallel-to-serial; MZM: Mach-Zehnder modulator; FFT: fast Fourier transform.

For the conventional method, the bit rate before coding was 12.04 Gb/s; 4.15% was used for the preamble, 2.88% for the pilot, and 2.88% for the CP. Taking into account the additional 7% for FEC coding, this resulted in a net transmission data rate of 10 Gb/s. For the two ICI self-cancellation methods, the bit rates was doubled in order to achieve the same net transmission data rate.

The effect of the proposed pilot-aided DFB loop is demonstrated in Fig. 3. The pilot-aided DFB loop not only compensated for the CPE caused by laser phase noise, but also eliminated the SPM caused by fiber nonlinearity. Figures 3(a) and (c) show that the CPE and the SPM could rotate the phase of all constellation points in a common direction; however, the difference could be seen in the phase rotation caused by CPE changes from an OFDM symbol to another. Figures 3(b) and (d) show that the proposed pilot-aided DFB loop effectively compensates for the phase rotation of the constellation point. In the simulations, optical signal-to-noise ratio (OSNR) was set to 30 dB.

Figure 4 shows the performance of zero-padding and data-conversion ICI self-cancellation schemes under large

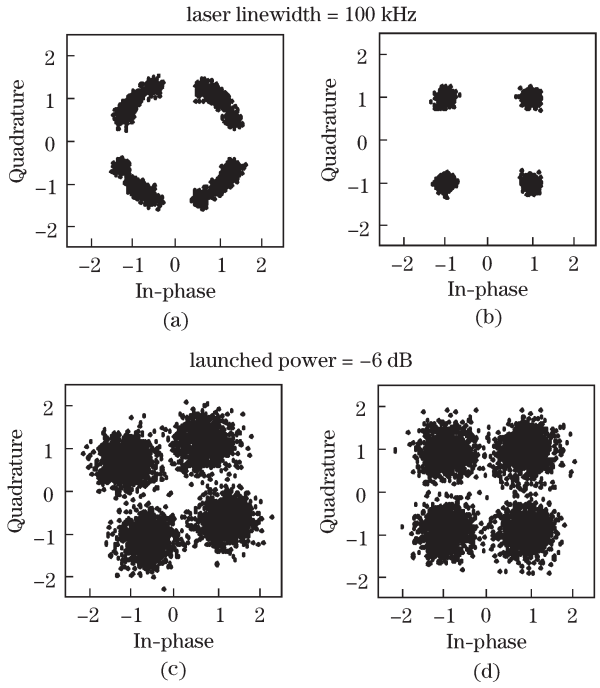

Fig. 3. Demonstration of the effect of the pilot-aided DFB loop: (a) under phase noise, without the loop; (b) under phase noise, with the loop; (c) under fiber nonlinearity, without the loop; (d) under fiber nonlinearity, with the loop.

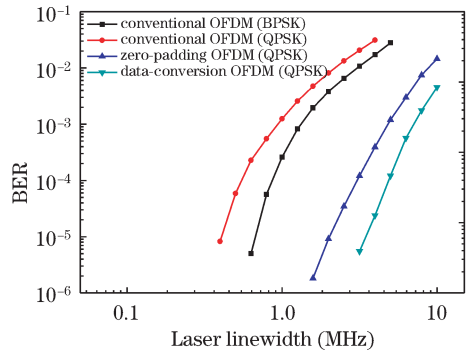

Fig. 4. Performance of the proposed schemes versus laser phase noise.

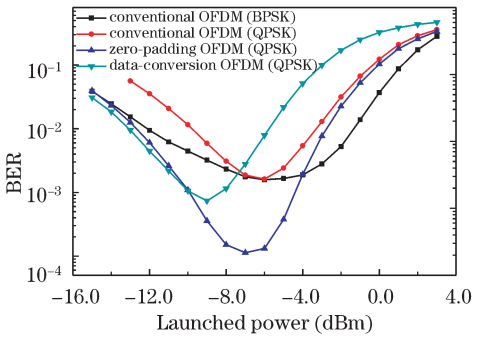

Fig. 5. Performance of the proposed schemes versus fiber nonlinearity.

laser linewidth. To evaluate the robustness of the proposed scheme against the phase noise contributed by the transmitter and receiver laser, the linewidth of the laser diodes (LDs) 1 and 2 was varied from 0.1 to 10 MHz. The data conversion scheme was most robust against laser phase noise. The two ICI self-cancellation schemes both performed better than the conventional CO-OFDM scheme. When the bit-error rate (BER) approached 10^{-6}, the tolerance of the conventional CO-OFDM scheme against the laser linewidth was around 300 kHz, whereas the two ICI self-cancellation schemes could work well with laser linewidth larger than 1 MHz.

Figure 5 shows the performance of zero-padding and data-conversion ICI self-cancellation schemes versus fiber nonlinearity. To demonstrate clearly the impact of fiber nonlinearity, the laser linewidth was set to 0 Hz during simulation. From Fig. 5, we can see that the systems with the ICI self-cancellation schemes obtain lower BER than the conventional CO-OFDM system. The zero-padding scheme significantly reduced inter-sub-carrier crosstalk on the effective sub-carrier. Consequently, the zero-padding scheme performed much better compared with the two others when fiber nonlinearity was considered.

The proposed scheme can be conveniently combined with other anti-interference techniques. For example, the impact of laser phase noise could be further depressed by combining the proposed scheme with the self-optical carrier extraction technique[16]. The fiber nonlinearity pre-compensation method could be introduced into the proposed scheme to make the CO-OFDM system more robust against fiber nonlinearity[21].

In conclusion, we investigate CO-OFDM schemes that integrate ICI self-cancellation and CPE compensation. The zero-padding scheme can suppress not only the ICI caused by laser phase noise, but also the inter-sub-carrier crosstalk caused by fiber nonlinearity. Although the data-conversion scheme performs better under large laser phase noise, it obtains less gain in terms of fiber nonlinearity. Thus, the zero-padding scheme is more applicable for practical CO-OFDM systems. Meanwhile, pilot-aided DFB loops can effectively compensate for both CPE and SPM. The proposed scheme can be conveniently combined with other anti-interference techniques to make the CO-OFDM system more robust against laser phase noise or fiber nonlinearity.

This work was supported by the National "973" Program of China (Nos. 2010CB328201 and 2010CB328202), the National Natural Science Foundation of China (Nos. 60907030, 60877045, 60932004, and 60736003), and the Scientific Research Foundation for the Returned Overseas Chinese Scholars.

References

1. J. H. Winters and R. D. Gitlin, IEEE Trans. Commun. **38,** 1439 (1990).
2. H. Bülow, F. Buchali, and A. Klekamp, J. Lightwave Technol. **26,** 158 (2008).
3. J. Armstrong, J. Lightwave Technol. **27,** 189 (2009).
4. W. Shieh, X. Yi, Y. Ma, and Q. Yang, J. Opt. Network. **7,** 234 (2008).
5. Z. Li, G. Hu, and L. Kong, Chinese J. Lasers (in Chinese) **35,** 582 (2008).
6. J. Zhang, K. Qiu, Y. Li, Y. Zhou, and H. Zhang, Acta Opt. Sin. (in Chinese) **29,** 323 (2009).
7. W. Shieh and C. Athaudage, Electron. Lett. **42,** 587 (2006).
8. W. Shieh, IEEE Photon. Technol. Lett. **19,** 134 (2007).
9. S. L. Jansen, I. Morita, T. C. W. Schenk, D. van den Borne, and H. Tanaka, in *Proceedings of OFC/NFOEC 2008* OMU3 (2008).
10. S. L. Jansen, I. Morita, T. C. W. Schenk, N. Takeda, and H. Tanaka, J. Lightwave Technol. **26,** 6 (2008).
11. Z. Tong, Q. Yang, Y. Ma, and W. Shieh, Electron. Lett. **44,** 1373 (2008).
12. A. Sano, E. Yamada, H. Masuda, E. Yamazaki, T. Kobayashi, E. Yoshida, Y. Miyamoto, R. Kudo, K. Ishihara, and Y. Takatori, J. Lightwave Technol. **27,** 3705 (2009).
13. S. Wu and Y. Bar-Ness, IEEE Trans. Commun. **52,** 1988 (2004).
14. C. Li, W. Hu, and T. Wang, in *Proceedings of IEEE 65th Vehicular Technology Conference VTC2007* 2305 (2007).
15. X. Yi, W. Shieh, and Y. Ma, J. Lightwave Technol. **26,** 1309 (2008).
16. S. L. Jansen, I. Morita, and H. Takeda, in *Proceedings of ECOC 2007* Tu.5.2.2 (2007).
17. L. Xu, J. Hu, D. Qian, and T. Wang, in *Proceedings of OFC/NFOEC 2008* OMU4 (2008).
18. K. Forozesh, S. L. Jansen, S. Randel, I. Morita, and H. Tanaka, in *Proceedings of Summer Topicals 2008* WC2.4 (2008).
19. A. J. Lowery, S. Wang, and M. Premaratne, Opt. Express **15,** 13282 (2007).
20. H. Bao and W. Shieh, Opt. Express **15,** 4410 (2007).

21. A. J. Lowery, IEEE Photon. Technol. Lett. **19,** 1556 (2007).
22. Y. Zhao and S. Häggman, IEEE Trans. Commun. **49,** 1185 (2001).
23. J. Zhang, R. Hermann, and P. Zhang, IEEE Trans. Broadcast. **50,** 97 (2004).
24. X. Yi, W. Shieh, and Y. Tang, IEEE Photon. Technol. Lett. **19,** 919 (2007).